

Unusual Hall Effect Anomaly in MnSi under Pressure

Minhyea Lee,^{1,*} W. Kang,² Y. Onose,³ Y. Tokura,^{3,4} and N. P. Ong¹

¹Department of Physics, Princeton University, Princeton, New Jersey 08544, USA

²Department of Physics, University of Chicago, Chicago, Illinois 60637, USA

³Department of Applied Physics, University of Tokyo, Tokyo 113-8656, Japan

⁴ERATO, JST, Spin Superstructure Project (SSS), Tsukuba 305-8562, Japan

(Received 19 November 2008; published 4 May 2009)

We report the observation of a highly unusual Hall current in the helical magnet MnSi in an applied pressure $P = 6\text{--}12$ kbars. The Hall conductivity displays a distinctive stepwise field profile quite unlike any other Hall response observed in solids. We identify the origin of this Hall current with the effective real-space magnetic field due to chiral spin textures, which may be a precursor of the partial-order state at $P > 14.6$ kbar. We discuss evidence favoring the chiral spin mechanism for the origin of the observed Hall anomaly.

DOI: 10.1103/PhysRevLett.102.186601

PACS numbers: 72.15.Gd, 72.25.Ba, 75.30.Kz, 75.45.+j

In the helical, itinerant magnet MnSi, a novel magnetic state with “partial order” has been reported by Pfleiderer and co-workers above a critical applied pressure $P_c = 14.6$ kbar [1–3]. The neutron diffraction intensity is broadly distributed over the surface of a sphere in momentum space, but is resolution limited in the radial direction. Several groups have proposed that the state harbors nontrivial topological spin textures [4–7]. We have observed a highly unusual Hall current in MnSi at pressures (6–12 kbar) just below P_c , which appears to be caused by fluctuations into the chiral-spin state at temperatures T near the Curie transition temperature T_C .

At ambient pressure, MnSi, which is noncentrosymmetric with the crystal structure B20, undergoes a transition at $T_C \approx 30$ K to a helical state with a long pitch $\lambda \sim 180$ Å. The wave vector \mathbf{q} is weakly pinned along the $\langle 111 \rangle$ direction. The helical state reflects the competition between the exchange energy and the Dzyaloshinsky-Moriya term [8–10]. In a magnetic field \mathbf{H} , \mathbf{q} shifts to alignment, and the helical state evolves to a conical magnetic state, whose cone angle steadily decreases to zero at a field $H_s \sim 0.6$ T. Under pressure, T_C decreases monotonically, reaching zero at the critical pressure $P_c \sim 14.6$ kbar (Fig. 1, inset). Above P_c , the “partial-order” state displays a non-Fermi liquid exponent in its resistivity [1] in addition to the unusual neutron diffraction spectrum.

The new Hall anomaly is observed in weak H in the pressure interval $6 < P < 12$ kbar below the curve of T_C vs P (shaded region in the inset of Fig. 1). Figure 1 (main panel) displays the Hall resistivity ρ_{yx} measured at several temperatures (T) with P fixed at 11.4 kbar ($T_C = 11.3$ K). At the lowest T (0.35 and 2.5 K), ρ_{yx} is holelike and H -linear. Between 5 and 10 K, however, we observe a prominent Hall anomaly with a most unusual profile. The steplike onset at the field $H_1 \sim 0.1$ T and the equally abrupt disappearance at $H_2 \sim 0.45$ T stands in sharp contrast with the broad background at higher H [the latter is

the *conventional* anomalous Hall effect (AHE) term common to all ferromagnets]. We show below that this unusual anomaly is the Hall-current response produced by coupling between the spin of charge carriers with chiral-spin textures. Its observation provides strong evidence that the

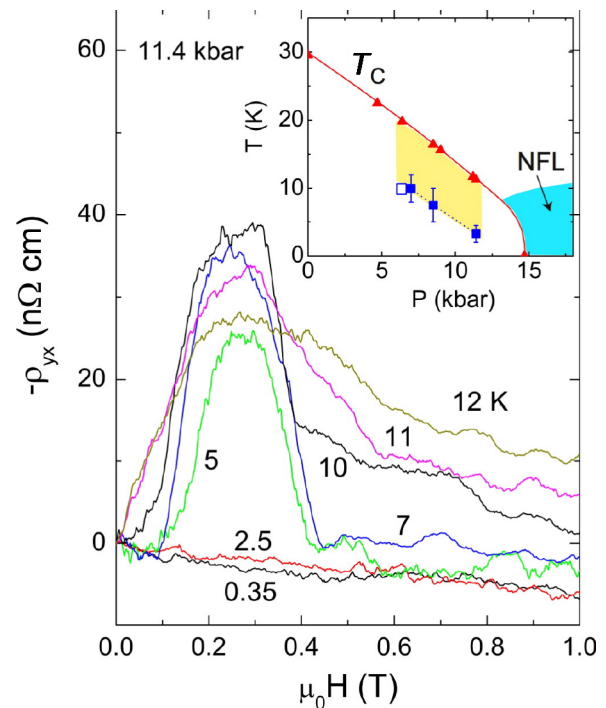


FIG. 1 (color online). (Main panel) Curves of $-\rho_{yx}$ in MnSi at 11.4 kbar revealing a large Hall anomaly in the field range $0.1 < H < 0.45$ T for several $T < T_C$ ($T_C = 11.3$ K), with \mathbf{H} nominally along $\langle 111 \rangle$. The anomaly (electronlike in sign) arises from a new contribution σ_{xy}^C to the total Hall conductivity. In the phase diagram (inset), the shaded region is where σ_{xy}^C is resolved. T_C was determined from ρ vs T . Data from Samples 1 and 2 are shown as solid and open squares, respectively. The non-Fermi liquid (NFL) region is shaded dark gray (adapted from Ref. [2]).

chiral-spin textures exist over a large fraction of the phase diagram for $P < P_c$.

Motivated by the results of Refs. [1–3], several groups [4–7] have proposed states comprised of crystalline arrays of magnetic textures. In Ref. [7], the transition at P_c is from a single-spiral state to a bcc “spin crystal” comprised of 6 spirals. In Refs. [4,5], the proposed state is either a square lattice configuration of topological defects called Skyrmion [4,5], or a cubic network of line defects which are double-twist configurations [5]. The textures are closely related to the defects previously studied in the blue phase of nematic liquid crystals [5,6].

Hall measurements were made in a ^3He cryostat using a miniature clamp-type pressure cell (13 mm dia.) made of BeCu alloy and tungsten carbide with Fluorinert (FC-77) as the pressure medium. At low T , the pressure was calibrated by the superconducting transition of a Pb coil detected by ac susceptibility. The high-purity MnSi crystals (of resistivity ratio $\rho(300\text{ K})/\rho(4.2\text{ K}) \approx 60$ and typical size $1.1 \times 0.5 \times 0.060\text{ mm}^3$) were cut from boules grown in a floating-zone furnace. The Hall voltage V_H was checked to scale linearly with current I (typically 0.5 to 1 mA). At each T and P , V_H was recorded with H swept at the rate 0.02 T/min. in the sequence $0 \rightarrow -1T \rightarrow 0 \rightarrow 1T \rightarrow 0$ to eliminate errors from induced emf’s and drifts in T . The observed Hall anomaly is always antisymmetric in H even without antisymmetrization of the 4 raw curves. Results obtained in the 2 crystals investigated are closely similar.

In ferromagnets, the observed Hall resistivity ρ_{yx} is the sum of the ordinary Hall resistivity $\rho_{yx}^N = \sigma_{xy}^N \rho^2$ and the AHE term $\rho_{yx}^A = \sigma_{xy}^A \rho^2$, where $\rho = \rho_{xx}$ is the resistivity and σ_{xy}^N and σ_{xy}^A are the ordinary and anomalous Hall conductivities, respectively. Dividing by ρ^2 , we have

$$\frac{\rho_{yx}}{\rho^2} = \sigma_{xy}^N + \sigma_{xy}^A. \quad (1)$$

The first term is strictly H linear in low H while the second term scales as the uniform magnetization $M(T, H)$.

To bring out the surprising nature of the new anomaly, we recall the salient features of the Hall Effect at ambient P [11,12]. In high-purity MnSi, Lee *et al.* [12] have shown that, in spite of the large magnetoresistance (MR), the H dependence of σ_{xy}^A at ambient P strictly mimics that of $M(T, H)$, *viz.* $\sigma_{xy}^A(T, H) = S_H M(T, H)$, with S_H a constant independent of T and H . This scaling confirms a key prediction of the Karplus-Luttinger (KL) theory [13] (and its generalization using the Berry phase [14–16]).

Returning to the Hall curves in MnSi under pressure, we plot in Fig. 2 curves of ρ_{yx} over a broader field range, with P fixed at 8.5 kbar (at which $T_C = 16.4\text{ K}$). Starting at 5 K, we observe that ρ_{yx} is linear in H to 7 T. This reflects the dominance of $\sigma_{xy}^N \sim \ell^2$ in the limit of large mean-free-path ℓ . With increasing T , however, the rapid increase of ρ strongly amplifies the anomalous term ρ_{yx}^A which emerges as a negative contribution with a broad shoulder (e.g., at

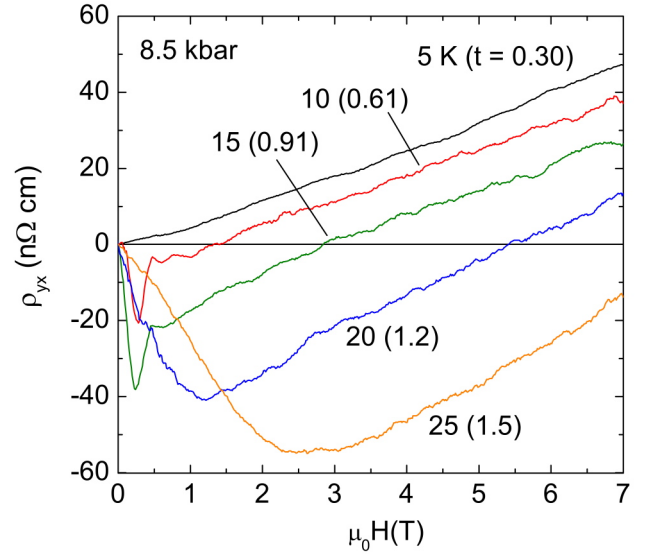


FIG. 2 (color online). Curves of ρ_{yx} extending to 7 T showing the relation of the Hall anomaly to other Hall terms (at the applied $P = 8.5\text{ kbar}$, $T_C = 16.4\text{ K}$). At 5 K, the holelike σ_{xy}^N dominates ρ_{yx} to produce an H -linear background. At $T = 10$ and 15 K, at which the Hall anomaly is observed as sharp negative spikes, the AHE term $\rho_{yx}^A = \sigma_{xy}^A \rho^2$ grows in prominence as ρ increases. Above T_C (20 and 25 K), the Hall anomaly vanishes, while ρ_{yx}^A continues to increase in magnitude. The reduced temperature $t = T/T_C$ is shown in parenthesis for each curve.

2.5 T at 25 K). We refer to this term as the “conventional” AHE term. At 10 and 15 K, we see the emergence of the new Hall anomaly as a sharp negative spike in weak fields. Raising T above T_C removes the spike (curves at 20 and 25 K). The curves above T_C are closely similar to those observed at ambient P (where the spike is absent).

The new Hall anomaly is qualitatively distinct from the Lorentz-force term and the KL term. As mentioned, theory predicts that coupling of the carrier spin to local textures of $\mathbf{M}(\mathbf{r})$ produces a large anomalous Hall current via the Berry phase [17,18]. In the past decade, the Berry-phase approach has greatly extended the purview of the KL theory [14–16]. In a periodic lattice, the “overlap” of wave functions $u_{\mathbf{k}}$ defines the Berry gauge potential $\mathbf{A}(\mathbf{k}) = \langle u_{\mathbf{k}} | i \nabla_{\mathbf{k}} | u_{\mathbf{k}} \rangle$, whose curl gives an effective magnetic field $\mathbf{\Omega}(\mathbf{k})$ that lives in \mathbf{k} space. When $\mathbf{\Omega}(\mathbf{k})$ is rendered finite (by breaking time-reversal invariance), it leads to orbit deflection in \mathbf{k} space, to reproduce the KL term σ_{xy}^A in Eq. (1).

Quite distinct from this strictly orbital coupling, the Berry phase can produce an *additional* effective magnetic field \mathbf{B}_ϕ via the spin degrees of freedom. The spin-mediated mechanism was initially invoked to explain AHE experiments in manganites [19] and pyrochlores [20]. We consider the simplest example in which the spins of a hopping electron aligns by Hund coupling J_H to the ion’s local moment \mathbf{S}_i at each site i [19,20]. As the electron

completes a closed loop linking 3 noncoplanar spins \mathbf{S}_i ($i = 1, 2, 3$), \mathbf{s} describes a cone of finite solid angle Ω_s (Fig. 3, inset). Hence, the electron acquires a Berry phase $\phi_B = \frac{1}{2}\Omega_s$, which translates to a magnetic field in real space $B_\phi = (\phi_B/2\pi)(\phi_0/\mathcal{A})$ that can be extremely large (\mathcal{A} is the loop area and ϕ_0 the flux quantum). For, e.g., even for $\Omega_s \sim \pi/100$ over an area $\mathcal{A} \sim 5 \times 5 \text{ \AA}^2$, we have $B_\phi \sim 42 \text{ T}$. In turn, \mathbf{B}_ϕ produces a large Hall conductivity σ_H^C that is proportional to the chirality $\chi_c = \mathbf{S}_1 \cdot \mathbf{S}_2 \times \mathbf{S}_3$ [17,18,20].

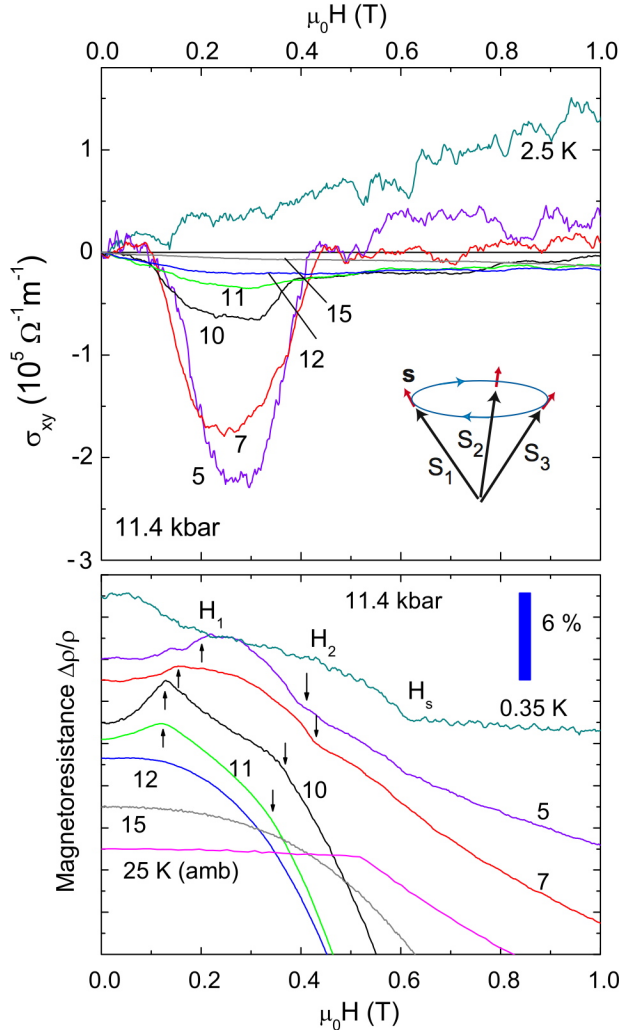


FIG. 3 (color online). Panel (a) Curves of σ_{xy} vs H at $P = 11.4 \text{ kbar}$ at selected T . The Hall anomaly σ_{xy}^C is prominent between 11 and 5 K between the fields H_1 and H_2 . At 2.5 K, only the normal term σ_{xy}^N is observed. The inset shows the itinerant spin \mathbf{s} aligned with the local moment \mathbf{S}_i on site i by a large J_H . As the electron closes the path 1-2-3-1, it acquires a Berry phase ϕ_B . Panel (b) Curves of the MR $\Delta\rho/\rho$ vs H at selected T at 11.4 kbar (curves are offset for clarity). Below T_C (11.3 K), anomalies indicate fields H_1 (up arrows), H_2 (down arrows), and H_s . By comparison, the MR is nearly zero below $H_s = 0.6 \text{ T}$ at ambient pressure (thin curve at 25 K).

The foregoing also applies to itinerant ferromagnets [18]. In a spiral helimagnet such as MnSi, the local spin direction $\mathbf{S}(\mathbf{r})$ varies periodically with a pitch set by the wave vector \mathbf{q} . For an itinerant electron, the exchange energy forces its spin \mathbf{s} to follow the spatial variation of $\mathbf{S}(\mathbf{r})$. However, as emphasized in Ref. [21], a spiral state with a single \mathbf{q} has zero chirality. In order to produce finite chirality, we must have a multi- \mathbf{q} spiral state, as has been proposed for the partial-order state for $P > P_c$.

In the novel states proposed [4–7], the presence of Skyrmion or double-twist configurations naturally leads to chirality. We expect σ_H^C to be proportional to the Skyrmion number $N_s = \int d^3r \Phi_z(\mathbf{r})$, with the Skyrmion density $\Phi_z = (8\pi)^{-1} \hat{\mathbf{n}} \cdot (\partial_x \hat{\mathbf{n}} \times \partial_y \hat{\mathbf{n}})$ and $\hat{\mathbf{n}} = \mathbf{S}(\mathbf{r})/|\mathbf{S}(\mathbf{r})|$.

For the region of our Hall experiment ($P < P_c$), we expect fluctuations towards the multi- \mathbf{q} state to be favorable at temperatures just below T_C (the fluctuations are strongly suppressed as $T \rightarrow 0$). Hence, within the broad swath in which σ_{xy}^C is observed (Fig. 1 inset), we propose that chirality exists caused by strong fluctuations into multi- \mathbf{q} helical states.

There is considerable evidence for strong fluctuations in the region $P < P_c$. The muon spin rotation data by Uemura *et al.* [22] show that, for $P < P_c$, magnetic order exists only in a partial volume fraction, in agreement with conclusions from nuclear magnetic resonance [23] and neutron scattering [24] experiments. In a broad range of P below P_c , strong fluctuations appear as a precursor to the partial-ordered state above P_c .

Within this picture, we may understand several puzzling features of the Hall data (as well as the MR). To examine these issues in more detail, we transform ρ_{yx} to $\sigma_{xy} = \rho_{yx}/\rho^2$ using the simultaneously measured curve of ρ vs H . As plotted in Fig. 3(a), the Hall anomaly is now apparent as a large Hall conductivity σ_{xy}^C , with a distinctive field profile. Just below T_C , the anomaly first appears as a shallow hull feature (compare curves at 12 and 11 K). With decreasing T , it deepens considerably. Comparing the curves of σ_{xy} with the MR curves, we see that σ_{xy}^C is restricted to the narrow interval $H_1 < H < H_2$. At 5 K, its magnitude is ~ 10 times larger than the other 2 Hall terms, and $\sim 1\%$ of the zero- H conductivity σ . Finally, at 2.5 K, the anomaly vanishes, leaving an H -linear background that is dominated by σ_{xy}^N .

We next discuss the evidence for the chiral-spin mechanism. First, we note that, between H_1 and H_2 , $|\sigma_{xy}^C|$ attains remarkably large values. At ambient pressure and at $T = 5 \text{ K}$ with $H = 0.3 \text{ T}$, the measured values of the ordinary term and the KL term, σ_{xy}^N and σ_{xy}^A , are $\sim +3.2 \times 10^4$ and $-1.2 \times 10^4 (\Omega \text{ m})^{-1}$, respectively [12]. By comparison, $|\sigma_{xy}^C|$ is 10 times larger than either of these values. Such a large σ_{xy}^N is difficult to understand with orbital mechanisms given the small values of H_1 and H_2 . By contrast, the chiral-spin term is easily capable of producing such a large Hall response. The effective field B_ϕ can exceed 40 T despite the small applied H .

Second, σ_{xy}^C is seen to be finite only within a very narrow field interval (H_1, H_2). The relatively abrupt vanishing of σ_{xy}^C at $H_2 \sim 0.45$ T is striking. Such an abrupt vanishing of the Hall current seems impossible to realize with orbital mechanisms (carrier mobilities cannot be abruptly changed in such weak H). By contrast, the spin Berry phase model applied to MnSi anticipates that σ_{xy}^C must vanish at a field below H_s , as the cone angle of the spiral state is suppressed to zero. In the ferromagnetic state above H_s , spin textures are energetically prohibitive. As the spin textures are removed with increasing H , σ_{xy}^C must vanish. Hence, H_s represents an upper bound for a finite σ_{xy}^C . The Hall results show that the vanishing actually occurs at the slightly lower field H_2 . The observed mesa profile of $\sigma_{xy}^C(H)$ has been reproduced in a recent calculation [21] based on the bcc1 “spin-crystal” ground state of MnSi.

Third, the picture described also clarifies the origin of the kink anomalies long known in MnSi under pressure [25]. The low- T transverse MR of MnSi is very large and negative throughout its phase diagram because of its long ℓ . Under pressure, weak anomalies appear at fields $H < H_s$. Figure 3(b) compares the transverse MR measured in our sample at ambient pressure and at 11.4 kbar with $\mathbf{H} \perp \mathbf{I}$ (applied current). First, we examine the MR curve at ambient P (lowest curve, at 25 K, with $T_C = 30$ K). Surprisingly, the MR is almost zero below H_s . A sharp kink at H_s signals saturation of the moments, followed by a steep decrease of ρ at larger H . The absence of MR implies that, as \mathbf{q} reorients in \mathbf{H} and the cone angle decreases [26], there is no change in the carrier scattering rate Γ in $H < H_s$ [12,25]. Consequently, the changes below H_s involve no change in magnetic disorder or the creation of spin defects at ambient P . The “rigidity” of the spiral state at ambient pressure also explains why the Hall anomaly is not observed at ambient pressure.

By contrast, at $P = 11.4$ kbar, the MR exhibits kinks in the interval $0 < H < H_s$. Above T_C (11.3 K), the MR decreases smoothly. At 11 K, the 2 field scales H_1 and H_2 inferred from σ_{xy} [Fig. 3(b)] become apparent (up and down arrows, respectively). Their positions change only slightly with T . However, they become more sharply defined as T approaches T_C from below. Throughout the interval $(0, H_s)$, the visible MR anomalies imply that changes in the magnetic structure are accompanied by the production of magnetic defects and textures which increase Γ . Hence, in both transport channels, the onset and disappearance of σ_{xy}^C at 11.4 kbar at H_1 and H_2 are nearly coincident with the MR anomalies.

Our experiment reveals that, when a charge current flows through a region with chiral-spin textures, a large Hall current appears. The spin-texture generated Hall current disappears if the textures are erased by increasing H . Because of the abruptness of its onset and disappearance in a narrow field interval, the new Hall conductivity σ_{xy}^C is easily distinguished from both the conventional AHE term and Lorentz-force term. Its distinctive profile suggests that

it may serve as a sensitive detector of chiral-spin textures in helical magnets. We find that, in MnSi, these textures exist over a significant region of the phase diagram below the T_C curve for $P < P_C$.

We thank B. Binz, A. Vishwanath, and M. Hermele for valuable discussions. The research at Princeton is supported by the U.S. National Science Foundation under MRSEC Grant No. DMR 0213706.

*Present address : National Institute of Standards and Technology, Boulder, CO 80305, USA.

- [1] C. Pfleiderer, S.R. Julian, and G.G. Lonzarich, Nature (London) **414**, 427 (2001).
- [2] C. Pfleiderer *et al.*, Nature (London) **427**, 227 (2004).
- [3] C. Pfleiderer, P. Böni, T. Keller, U.K. Rössler, and A. Rosch, Science **316**, 1871 (2007).
- [4] U.K. Rössler, U.N. Bogdanov, and C. Pfleiderer, Nature (London) **442**, 797 (2006).
- [5] I. Fischer, N. Shah, and A. Rosch, Phys. Rev. B **77**, 024415 (2008).
- [6] S. Tewari, D. Belitz, and T.R. Kirkpatrick, Phys. Rev. Lett. **96**, 047207 (2006).
- [7] B. Binz, A. Vishwanath, and V. Aji, Phys. Rev. Lett. **96**, 207202 (2006); B. Binz and A. Vishwanath, Phys. Rev. B **74**, 214408 (2006).
- [8] Y. Ishikawa and M. Arai, J. Phys. Soc. Jpn. **53**, 2726 (1984).
- [9] *Spin Fluctuation in Itinerant Electron Magnetism*, edited by T. Moriya, Springer Series in Solid-State Sciences (Springer, Berlin (1985), and references therein.
- [10] C. Pfleiderer, G.J. McMullan, S.R. Julian, and G.G. Lonzarich, Phys. Rev. B **55**, 8330 (1997).
- [11] N. Manyala, *et al.* Nature Mater. **3**, 255 (2004).
- [12] M. Lee, Y. Onose, Y. Tokura, and N.P. Ong, Phys. Rev. B **75**, 172403 (2007).
- [13] R. Karplus and J.M. Luttinger, Phys. Rev. **95**, 1154 (1954).
- [14] Ganesh Sundaram and Qian Niu, Phys. Rev. B **59**, 14915 (1999).
- [15] M. Onoda and N. Nagaosa, J. Phys. Soc. Jpn. **71**, 19 (2002).
- [16] T. Jungwirth, Qian Niu, and A.H. MacDonald, Phys. Rev. Lett. **88**, 207208 (2002).
- [17] J. Ye *et al.*, Phys. Rev. Lett. **83**, 3737 (1999).
- [18] Gen Tatara and Hikaru Kawamura, J. Phys. Soc. Jpn. **71**, 2613 (2002).
- [19] P. Matl *et al.*, Phys. Rev. B **57**, 10248 (1998).
- [20] Y. Taguchi, Y. Oohara, H. Yoshizawa, N. Nagaosa, and Y. Tokura, Science **291**, 2573 (2001).
- [21] B. Binz and A. Vishwanath, Physica B (Amsterdam) **403**, 1336 (2008).
- [22] Y.J. Uemura *et al.*, Nature Phys. **3**, 29 (2007).
- [23] W. Yu *et al.*, Phys. Rev. Lett. **92**, 086403 (2004).
- [24] B. Fåk, R.A. Sadykov, J. Flouquet, and G. Lapertot, J. Phys. Condens. Matter **17**, 1635 (2005).
- [25] K. Kadowaki, K. Okuda, and M. Date, J. Phys. Soc. Jpn. **51**, 2433 (1982).
- [26] Y. Ishikawa, G. Shirane, J. A. Tarvin, and M. Kohgi, Phys. Rev. B **16**, 4956 (1977).